A PROTEOMIC PROFILE OF IMIDACLOPRID AND ITS ACTIVE METABOLITES DESNITRO-IMIDACLOPRID AND IMIDACLOPRID-OLEFIN IN HUMAN NEURAL CELLS.

Sreehari Girish Kumar

A Thesis
Submitted to the
Graduate Faculty
of
George Mason University
in Partial Fulfillment of
The Requirements for the Degree
of
Master of Science
Biology

Committee:

_____	Dr. Nadine Kabbani, Thesis Chair
_____	Dr. James L. Olds, Committee Member
_____	Dr. Karl Fryxell, Committee Member
_____	Dr. Iosif Vaisman, Director, School of Systems Biology
_____	Dr. Donna Fox, Associate Dean, Office of Student Affairs & Special Programs, College of Science
_____	Dr. Fernando R. Miralles-Wilhelm Dean, College of Science
Date: _____	Summer Semester 2022 George Mason University Fairfax, VA

A Proteomic Profile of Imidacloprid and its Active Metabolites Desnitro-Imidacloprid and Imidacloprid-Olefin in Human Neural Cells.

A Thesis submitted in partial fulfillment of the requirements for the degree of Master of Science at George Mason University

by

Sreehari Girish Kumar
Bachelor of Science in Neuroscience
George Mason University, 2020

Director: Nadine Kabbani, Associate Professor
School of Systems Biology

Summer Semester 2022
George Mason University
Fairfax, VA

DEDICATION

This is dedicated to my family, who helped me get through my academic journey and achieve my personal and professional goals.

ACKNOWLEDGEMENTS

I would like to thank my committee chair, Dr. Kabbani, and committee members, Dr. Olds and Dr. Fryxell, for helping me throughout the development, research and writing aspects of my thesis project.

TABLE OF CONTENTS

LIST OF TABLES

LIST OF FIGURES

ABSTRACT

A PROTEOMIC PROFILE OF IMIDACLOPRID AND ITS ACTIVE METABOLITES DESNITRO-IMIDACLOPRID AND IMIDACLOPRID-OLEFIN IN HUMAN NEURAL CELLS.

Sreehari Girish Kumar, M.S.

George Mason University, 2022

Thesis Director: Dr. Nadine Kabbani

Neonicotinoids are a popular class of pesticides around the world and have been shown to bind both insect and mammalian nicotinic acetylcholine receptors (nAChRs). Imidacloprid (IMI), is amongst the most commonly used neonicotinoids in agriculture and domestic, non-industrial, applications but shows strong toxic effects in many organisms. In addition, the potential for toxicity from its two main metabolites desnitro-imidacloprid (DN-IMI) and imidacloprid-olefin (IMI-olefin), are not yet defined despite recent evidence that they can bind to the mammalian nAChR. In this study, we used Lund Human Mesencephalic (LUHMES) cells, as a human cell line model of dopaminergic neurons to test the effects of IMI and its metabolites. Cells were treated with 50μM IMI, DN-IMI, and IMI-olefin for 48 hours, and then examined for proteomic change using liquid-chromatography electrospray ionization mass spectrometry (LC-ESI MS/MS). Bioinformatic analysis using Gene Ontology (GO) and enrichment analysis were

performed using the Kyoto Encyclopedia of Genes and Genomes (KEGG), Reactome, and WikiPathways databases. Our results provide novel insight into convergent as well as differential molecular effects by IMI, DN-IMI, and IMI-olefin in neural cells. These studies begin to explore pathways of neonicotinoid neurotoxicity leading to neuro disease in exposed individuals.

CHAPTER ONE-INTRODUCTION

Neonicotinoids (neonics) have become the most widely used class of pesticides in the world replacing more dangerous compounds such as organophosphates. Imidacloprid (IMI) is the first commercially available neonic first introduced in the 1990s and is still amongst the most commonly used in more than 120 countries **[4,15,23]**. In 2014, over two million kg of IMI were used agriculturally in the United States (excluding Hawaii and Alaska) on pasture, hay, alfalfa, orchards, grapes, rice, vegetables, fruit, cotton, wheat, soybeans, corn, and other crops **[42].** Neonics are systemic, taken up by the plant during application, and maintain long-half lives, and cannot be removed by washing **[15]**. Neonics such as IMI can also be found in household pesticides and flea/tick control treatments in domestic animals that are in regular contact with humans **[10]**. Thus, neonics are pervasive chemical agents in both agricultural **[6,42]** and urban settings **[18]**, and are a concern for public safety and human health **[1,3,5,11,16,20,24,25,39]**. Studies show that neonics are readily detectable in human biosamples **[10,19,22,34,44,45,46]**.

Neonics share structural similarity to nicotine designed with an ability to bind with a high affinity at the insect nicotinic acetylcholine receptor (nAChR) target site **[16,23,27]**. However, studies show that neonics such as IMI, clothianidin, acetamiprid, and thiacloprid can also bind and activate non-insect, mammalian nAChRs **[41].** In

mammalian cells, neonics are found to activate several brain-type nAChR including α4β2, α7, and α3β4 nAChR subtypes **[4,13,24,25,40]**. These nAChR subtypes are expressed in both the developing and the adult brain and regulate important brain functions including cognition, attention, memory, and movement through synaptic mechanisms of neurotransmitter release. Nicotinic receptors are important in neurodegenerative diseases such as Alzheimer's and Parkinson's, and in developmental disorders such as ADHD and autism **[5],** and studies suggest that neonic toxicity may contribute to human neuro disease.

Various neonics are readily metabolized in the environment as well as within the organism upon ingestion through rapid enzymatic reactions involving reduction, oxidation, olefin formation, hydrolysis, chlorination, and demethylation **[24,39]**. In some cases, the metabolite is more toxic than the parent compound **[24,39]**. In the case of IMI, metabolism through cytochrome P450 and aldehyde oxidase has been shown to yield two pharmacologically active metabolites with an ability to activate mammalian nAChRs: desnitro-IMI (DN-IMI) and IMI-olefin **[7,24,32,33,38].** DN-IMI and IMI-olefin have been detected in various agricultural products as well as drinking water **[18,19,24,42**]. Studies show detectable amounts of DN-IMI and IMI-olefin in human urine (0.0020 μM DN-IMI and 0.0027 μM IMI-olefin) **[22,46]**. In experimental mouse models, DN-IMI appears able to cross the blood-brain barrier **[8]**, and pharmacological studies show that DN-IMI has an unusually high affinity for mammalian nAChRs comparable to that of

nicotine **[24,40]**. IMI-olefin has been found to be at least 10 times more potent than IMI in insects **[29]** and in a similar range as IMI in human cells **[24]**.

In this study, we examined the effects of IMI and its key metabolites, DN-IMI, and IMI-olefin on neuronal signaling in the human neuronal precursor lund human mesencephalic (LUHMES) cell line using proteomics. LUHMES cells are dopaminergic neurons that endogenously express nAChRs and have been used as a cellular model for studying molecular mechanisms of Parkinson's disease **[49]**. In recent studies, IMI, DN-IMI, and IMI-olefin have been shown to pharmacologically activate the nAChR leading to calcium signaling in LUHMES cells **[24,25]**. We used a combination of whole cell proteomics and informatics approach as described in **Figure 1** to find pathways and potential toxicity mechanisms associated with these neonics in neural cells.

.

CHAPTER 2-METHODS

2.1 Cell Culture

LUHMES cells were cultivated as previously described **[21,24,30,31]**. Briefly, LUHMES cells were grown in cell culture flasks (Sarstedt) precoated with 50 µg/ml poly-L-ornithine (PLO) and 1 µg/ml fibronectin (Sigma-Aldrich) in proliferation media (advanced DMEM/F12 (Gibco) with 2 mM L-glutamine (Sigma Aldrich), 1x N2-supplement (Gibco), and 40 ng/ml recombinant human basic fibroblast growth factor (FGF-2, R&D Systems)) at 37 °C and 5% CO_2. At passage 18, cells were differentiated in advanced DMEM/F12 media (Gibco) with 2 mM L-glutamine (Sigma Aldrich), 1x N2-supplement (Gibco), 1 mM N6,2'-0-dibutyryl 3',5'-cyclic adenosine monophosphate (cAMP) (Sigma Aldrich), 1 µg/ml tetracycline (Sigma Aldrich), and 2 ng/ml recombinant human glial cell-derived neurotrophic factor (GDNF, R&D Systems) for 48 hours. Cells were then plated at a density of 2.5 x 10^6 cells per well on 0.1% PEI-coated 6-well plates (Costar, Corning) for 7 days, exchanging 50% of the medium every 2-3 days.

At 9 days in vitro (DIV), cells were treated with 50 µM IMI, DN-IMI, or IMI-olefin (Sigma Aldrich) dissolved in DMSO while control cells were treated with DMSO only. After 48 hours, cells were lysed for proteomic analysis as described in **[36]**. Briefly, cells were washed in phosphate-buffered saline (PBS) and then detached using a cell

scraper. Cell fractions were centrifuged for 5 min at 500 x *g* at 4°C, and the pellet was resuspended in a solubilization buffer ([mM]: 20 Tris HCl (Carl Roth), 137 NaCl (Carl Roth), 2 EDTA (Sigma Aldrich), 10% glycerol (Carl Roth), 0.1% Triton X-100 (Sigma Aldrich), phosphatase inhibitor (PhosSTOP, Roche, Sigma Aldrich), and protease inhibitor (cOmplete, Roche, Sigma Aldrich). Protein concentrations were quantified using the Bradford assay. The sample was centrifuged for 20 min at 12,000 x *g* at 4°C and the supernatant was collected and stored at -80°C until proteomic analysis.

2.2 Cell Viability

LUHMES cells were plated on a 6-well plate and then treated with 50 µM IMI, DN-IMI, or IMI-olefin for 48 hours to replicate the experimental condition. Cells were incubated for 1 hour, at RT, and in the dark with Calcein AM (Invitrogen; C3100MP) or propidium iodide, (Sigma; P4170) in order to label live or dead cells, respectively. Cells were washed in PBS and then covered with imaging solution ([mM]: 140 NaCl, 4 KCl, 1 $MgCl_2$, 1.8 $CaCl_2$, 10 HEPES, 10 D-glucose, pH 7.4). Images were captured using the Cell Observer (Carl Zeiss Microscopy). Fluorescently labeled cells were quantified using Fiji ImageJ (version 1.53k) using Bernsen's thresholding method **[28]**.

2.3 Proteomics

Whole-cell proteomic analysis was performed as previously described **[36]**. Briefly, 100 µg of solubilized protein was precipitated with 4°C acetone for 5 minutes and then centrifuged for 2 minutes at 16,000 x *g* at 4°C. The protein pellet was air-dried for 1 min and then resuspended in 8M urea for sonication. The sample was then reduced using 1M DL-Dithiothreitol (DTT) for 5 min at 52°C and then digested by the addition of 0.01 µg/µL in trypsin for 4 hours at 37°C. Samples were purified using C-18 ZipTips (Millipore) and then reconstituted with 0.1% formic acid for analysis with liquid-chromatography electrospray ionization mass spectrometry (LC-ESI MS/MS) using an Exploris Orbitrap 480 coupled to an EASY-nLC 1200 HPLC system (Thermo Fisher Scientific, Waltham, MA, USA) C18 LC column (Thermo Fisher Scientific, Waltham, MA, USA) at a flow rate of 300 nL/min. Each sample was run 5 times. Proteins were identified using Proteome Discoverer *v*2.4 (Thermo Fisher Scientific, Waltham, MA, USA) and the SEQUEST HT search engine of MS spectra of the human NCBI 3-31-2018 database with the following parameters: mass tolerance for fragment ions = 5 ppm; mass tolerance for fragment ions = 0.05 Da; and cut-off value for the false discovery rate (FDR) in reporting peptide spectrum matches (PSM) to the database = 1%. Peptide abundance ratios and p-values were calculated via precursor ion quantification in Proteome Discoverer *v*2.4.

2.4. Bioinformatic Analysis

Proteins identified in at least 3 out of the 5 replicated samples were included in the proteomic analysis **[36].** Relative change in peptide abundance was determined using a label-free protein abundance ratio (fold-change) measure using the control (DMSO) as the reference **[36].** All peptide values were determined for statistical significance at $p < 0.05$. Proteomes were bioinformatically analyzed using Database for Annotation, Visualization, and Integrated Discovery (DAVID) (https://david.ncifcrf.gov/home.jsp, accessed 13 April 2022 through 6 June 2022) for gene ontology (GO) associations. In addition, Gene Enrichment Analysis (GEA) was performed against the Kyoto Encyclopedia of Genes and Genomics (KEGG), WikiPathways, and Reactome pathway databases in DAVID.

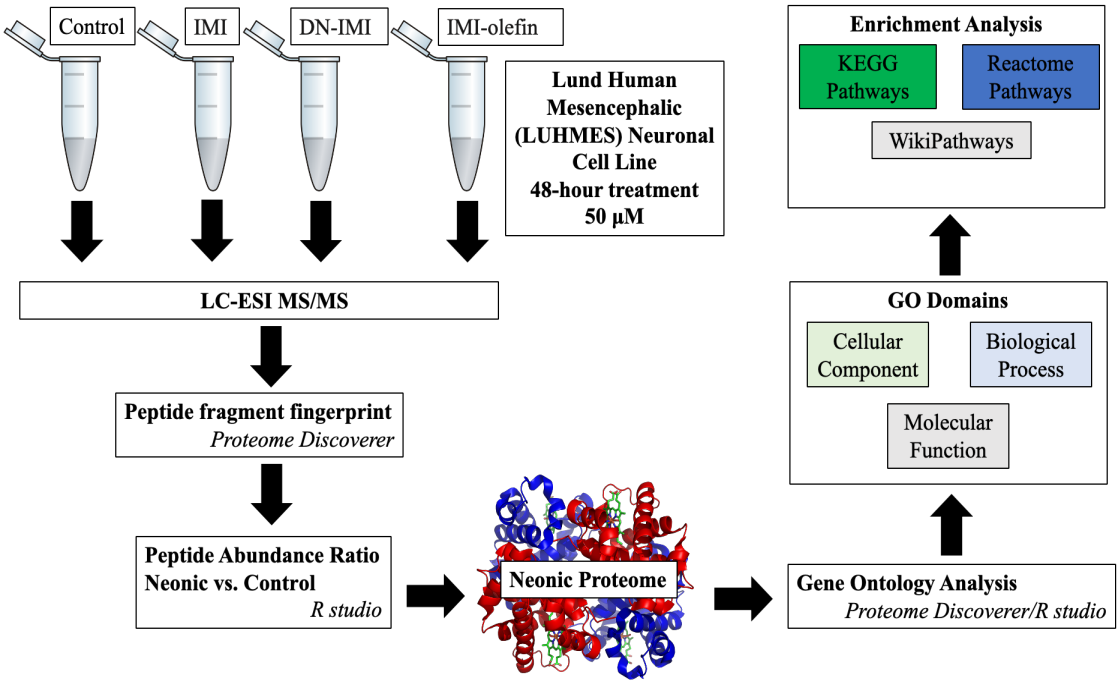

Figure 1: A summary flowchart of the experiment showing treatment conditions and mass spectrometry (LC-ESI MS/MS) coupled to bioinformatics using GO and enrichment analysis.

CHAPTER 3-RESULTS

3.1. Proteome Analysis of IMI-treated LUHMES cells

MS analysis of IMI-treated LUHMES cells identified a total of 3161 proteins for both control and IMI-treated cells. Out of the list of total number of proteins, 97 proteins were found to be differentially expressed within the IMI proteome relative to the vehicle control condition. These differentially altered proteins (aka IMI proteome) are subdivided into 68 upregulated and 29 downregulated proteins **(Figure 2).**

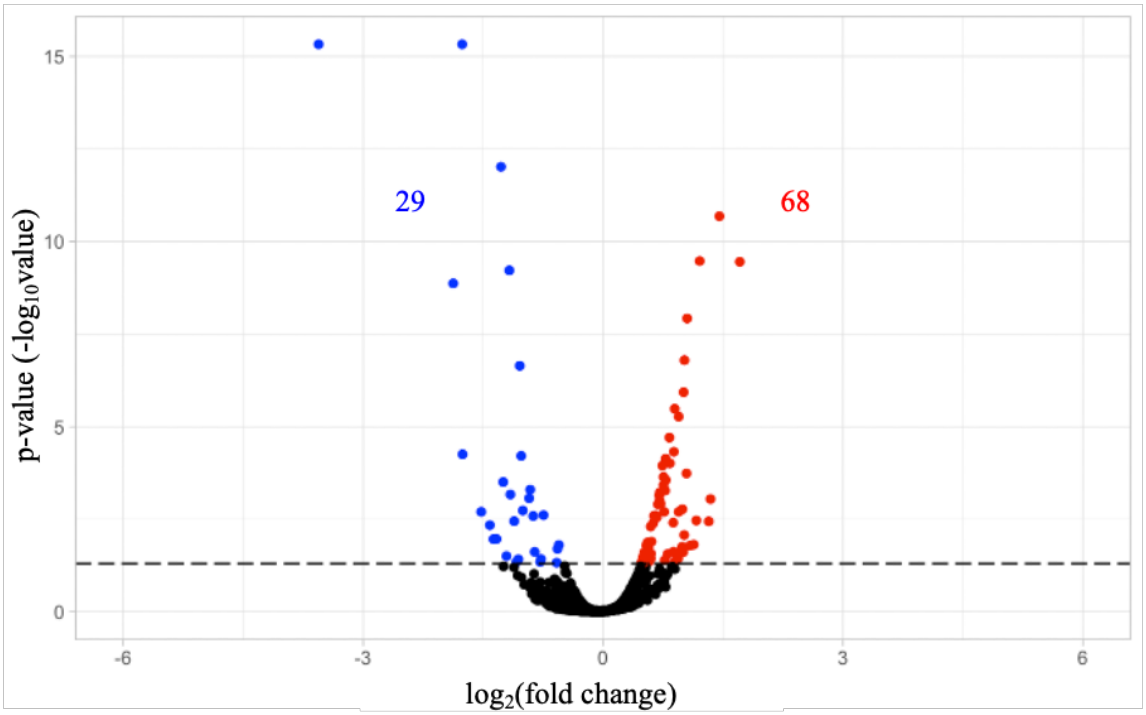

Figure 2: Volcano plot showing the distribution of differentially expressed proteins in IMI-treated LUHMES cells relative to controls. Each dot represents one of the 3161 proteins found in the MS sample. The blue dots (left) and red dots (right) show downregulated and upregulated proteins, respectively. The dotted line represents the threshold for statistical significance.

3.2. GO annotations and enrichment analysis of IMI proteome

GO annotations analysis illustrated that the most significant annotation affected in the GO domains of molecular functions, biological processes, and cellular components for IMI-treated LUHMES cells were “protein binding”, “protein transport” and “cytosol” respectively **(Figure 3A-C)**. Within protein binding 55 and 19 proteins were upregulated

and downregulated, respectively **(Figure 3A)**. In protein transport, the number of upregulated and downregulated proteins were 3 and 3, respectively **(Figure 3B)**. In the cytosol, 33 and 13 proteins were upregulated and downregulated, respectively **(Figure 3C)**. A GO domain pathway enrichment analysis illustrated that the highest enrichment occurs in protein binding and cytosolic expression consistent with GO annotation results **(Figure 3D)**.

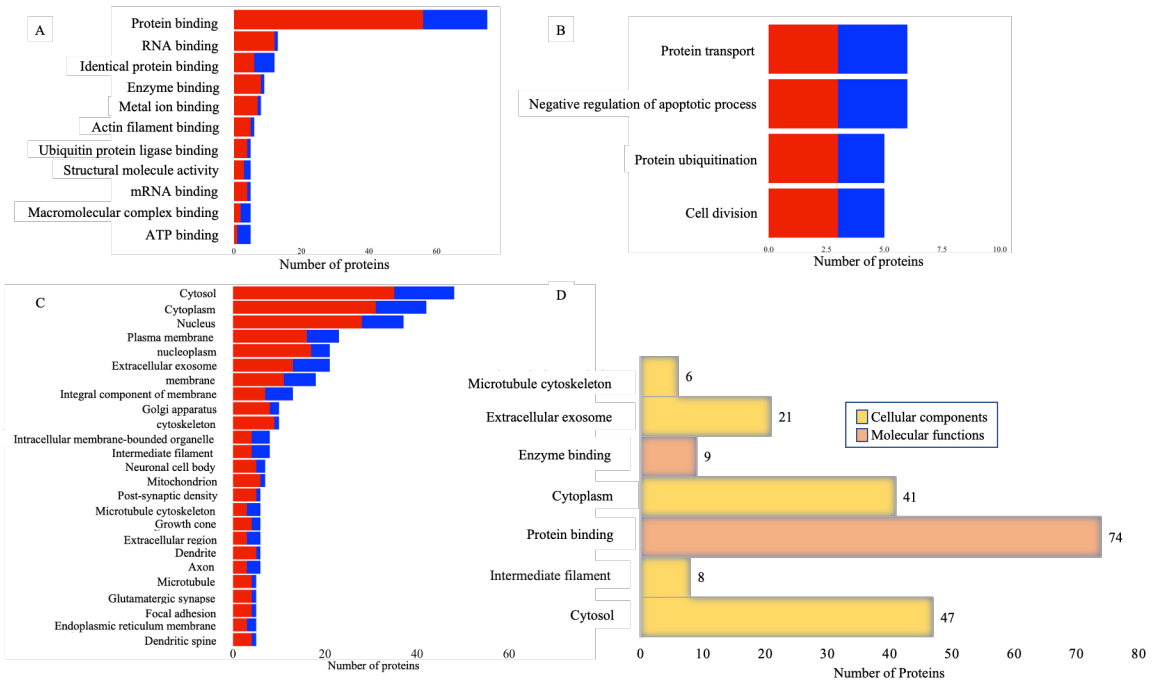

Figure 3: GO domains affected by IMI treatment of LUHMES cells. Total number of differentially expressed proteins categorized by (A) molecular function, (B) biological processes, and (C) cellular components. (D) Enrichment analysis of GO domains within the differentially expressed IMI proteome.

3.3. Proteome Analysis of DNI-IMI treated LUHMES cells

MS analysis of DN-IMI-treated LUHMES cells identified a total of 4787 proteins within the dataset. Out of these proteins, 109 proteins were found to be differentially expressed within the DN-IMI proteome relative to vehicle-treated controls. Within these differentially expressed proteins, 63 were downregulated while 46 proteins were upregulated **(Figure 4).**

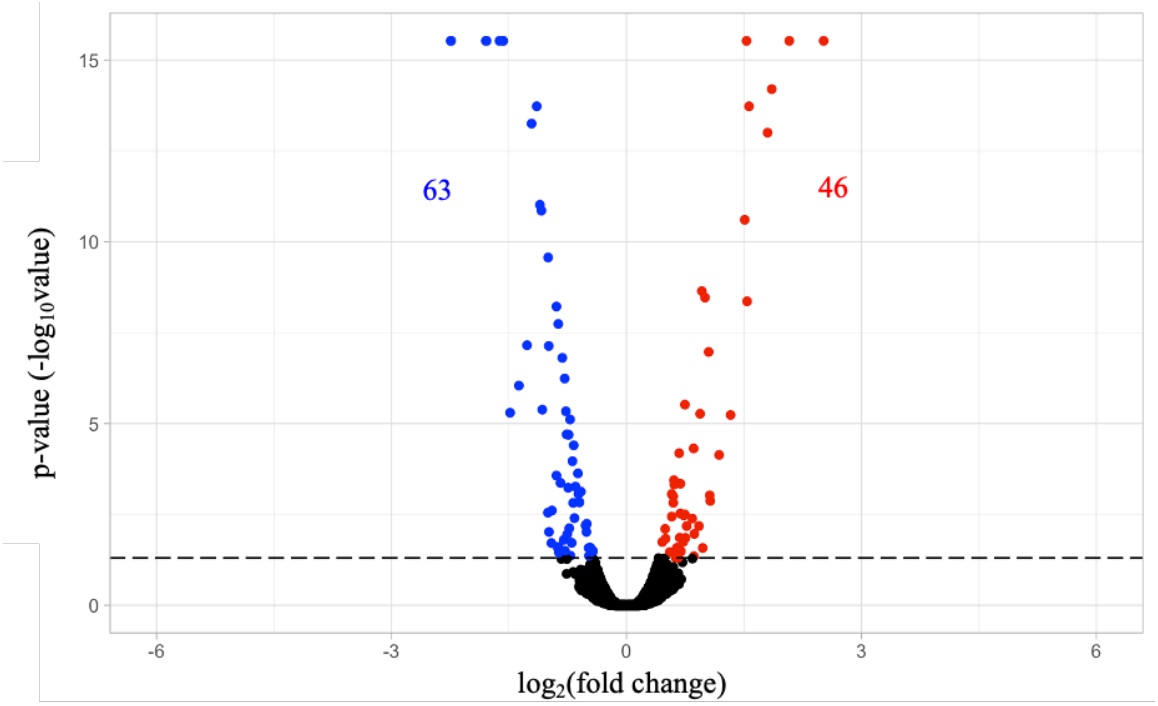

Figure 4: Volcano plot showing the distribution of differentially expressed proteins in DN-IMI treated LUHMES cells. Blue dots (left) and red dots (right) represent significantly downregulated and upregulated proteins within the DN-IMI treatment condition, respectively. The dotted line indicates the threshold for statistical significance.

3.4. GO annotations and enrichment analysis of DN-IMI proteome

GO annotations analysis illustrated that the most significantly affected GO domains within the molecular function, biological processes, and cellular components for significantly altered proteins within the DN-IMI treatment group. Specifically, GO analysis indicates that “protein binding”, “positive regulation of transcription from RNA polymerase II promoter” and “nucleus” respectively are significantly impacted **(Figure**

5A-C). Within protein binding, 33 proteins were upregulated in response to DN-IMI treatment **(Figure 5A)**. Within positive regulation of transcription from RNA polymerase II promoter, 3 proteins were upregulated and 7 downregulated in connection with DN-IMI **(Figure 5B)**. Within positive regulation of transcription from RNA polymerase II promoter, all of the 5 differentially regulated proteins associated with "cell proliferation" and "apoptotic process" annotations respectively were downregulated. 26 and 27 proteins out of the differentially expressed proteins were upregulated and downregulated respectively within the cytosol **(Figure 5C)**. GO domain pathways enrichment analysis indicates a high enrichment of protein binding and nuclear localization within the DN-IMI treatment dataset **(Figure 5D)**.

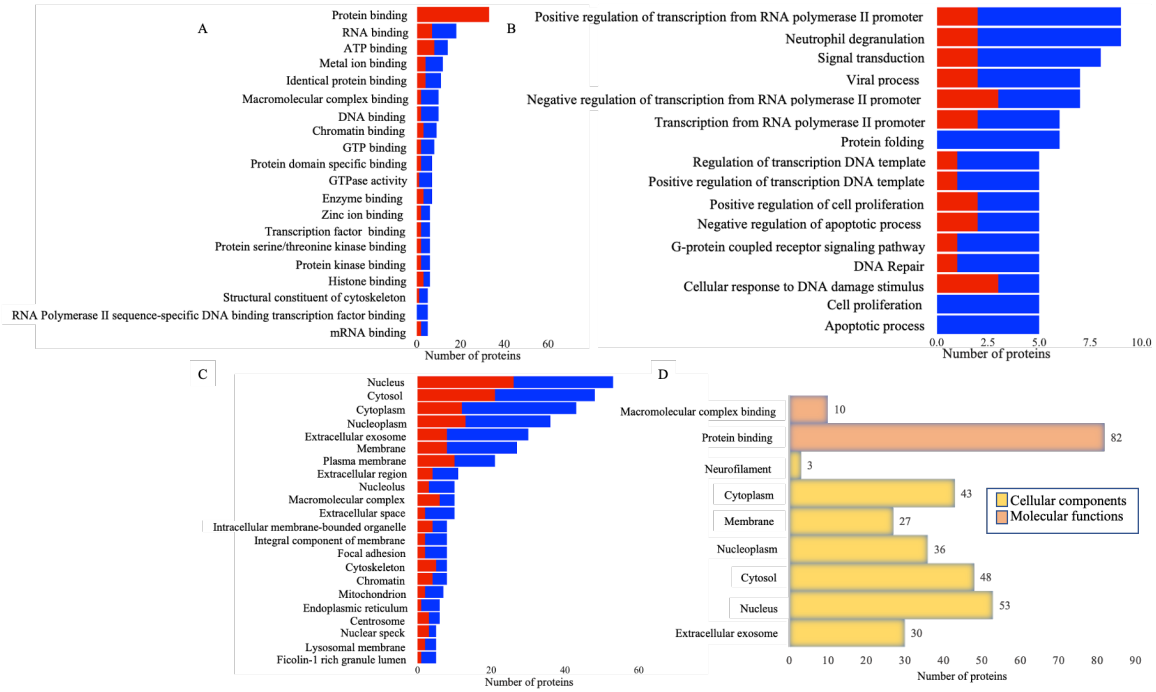

Figure 5: GO domains affected by DN-IMI treatment of LUHMES cells. Total number of differentially expressed proteins categorized by (A) molecular functions (B) biological processes and (C) cellular components. (D) Enrichment analysis of GO domains affected by the differentially expressed proteins within DN-IMI treated cells.

3.5. Pathway enrichment analysis of DN-IMI treated LUHMES cells

Enrichment analysis using the database of pathways from Reactome revealed that the differential expressed proteins within DN-IMI treated cells were enriched in Wnt pathway, nuclear receptor, G protein beta gamma, glutamate activated kainate receptor, and estrogen signaling receptor (ESR)- mediated signaling **(Figure 6)**. Within the (beta-catenin independent) Wnt signaling pathway, 5 out of the 7 and 8 out of 11 differential

expressed proteins were downregulated while RAC3, CALM2, and AKT2 proteins were upregulated **(Figure 6A)**. Out of the downregulated proteins in Wnt signaling, 7 out of 10 differential expressed proteins were downregulated while AKT2, CALM2, and POLR2L proteins were upregulated in nuclear receptor and ESR-mediated signaling **(Figure 6A)**. In glutamate-activated kainate receptor signaling, all of the differentially expressed proteins implicated within the pathway were downregulated except for CALM2 protein **(Figure 6A)**. All differentially expressed proteins involved in the pathway except for AKT2 protein were downregulated in G protein beta gamma signaling **(Figure 6A)**. Finally, all differentially expressed proteins associated with the corticotropin-releasing hormone signaling pathway and 5 out of 8 differentially expressed proteins implicated in Ras signaling pathway were downregulated while AKT2, RAC3, and CALM2 proteins were downregulated **(Figure 6B)**.

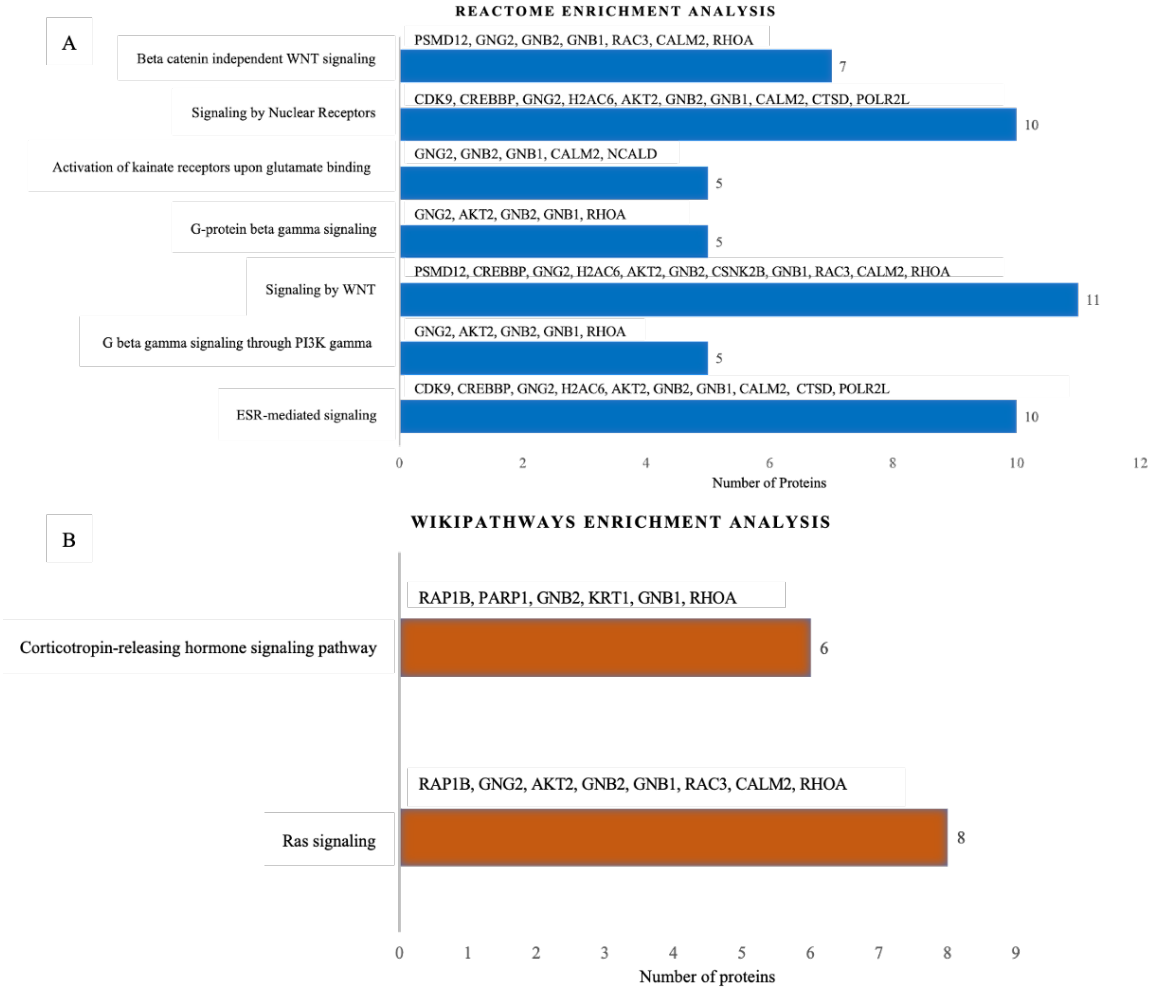

Figure 6: Pathway enrichment analysis of DN-IMI treated LUHMES cells. (A) Reactome pathways analysis. (B) WikiPathways analysis. The number and name of proteins within each component pathway is indicated.

3.6. Proteome Analysis of IMI-olefin treated LUHMES cells

MS analysis of IMI-olefin-treated LUHMES cells identified a total of 4787 proteins within the dataset, and out of these only 111 were found to be statistically

impacted by IMI-olefin treatment compared to controls. The IMI-olefin proteome consists of 56 upregulated and 55 downregulated proteins **(Figure 7).**

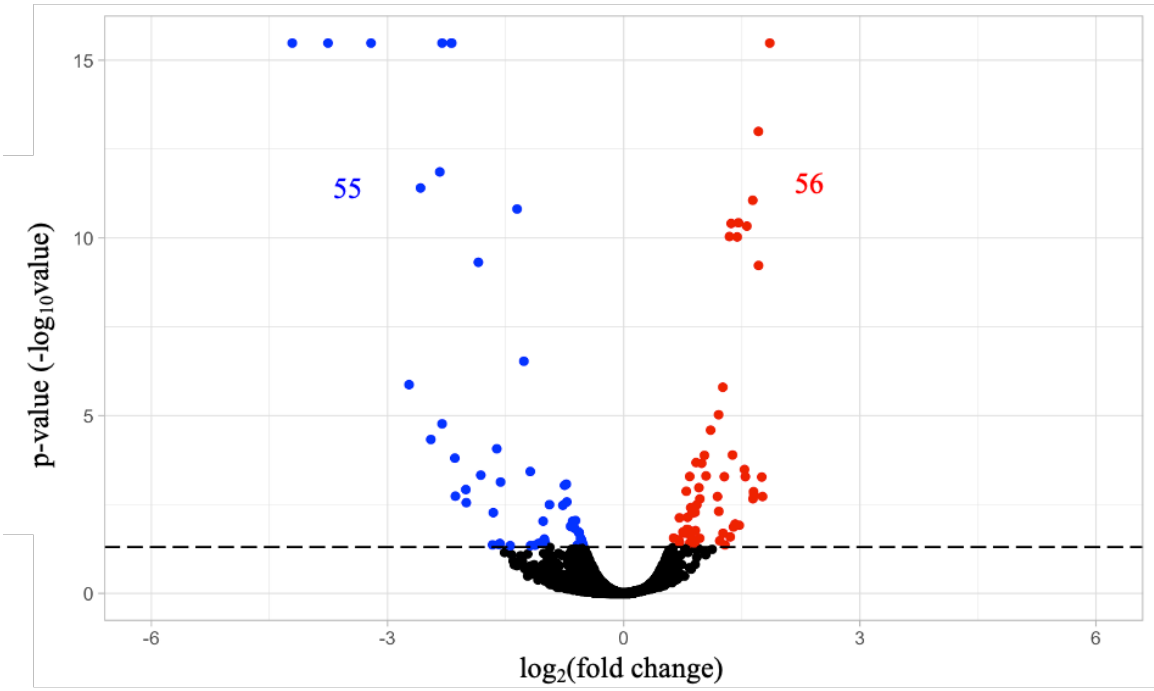

Figure 7: Volcano plot showing the distribution of differentially expressed proteins in IMI-olefin treated LUHMES cells. Each dot represents a protein. The blue dots (left) and red dots (right) show downregulated and upregulated proteins relative to controls. The dotted line represents the threshold for statistical significance within the dataset.

3.7. GO annotations and enrichment analysis of IMI-olefin proteome

GO annotations analysis illustrated that the most significant effects for IMI-olefin were "protein binding", "positive regulation of transcription from RNA polymerase II promoter" and "cytosol" respectively **(Figure 8A-C)**. Within protein binding 31 and 44

proteins were significantly downregulated and upregulated, respectively **(Figure 8A)**. In positive regulation of transcription from RNA polymerase II promoter, 5 proteins were upregulated and 3 downregulated **(Figure 8B)**. In positive regulation of transcription from RNA polymerase II promoter, "cytoplasmic translation", "translation" and "actin filament organization" are found to be most impacted **(Figure 8B)**. Specifically, 7 out of 8 differentially cytoplasmic translation proteins were downregulated, while all of the differentially expressed proteins impacted in "translation" were downregulated **(Figure 8B)**. In actin filament organization, 6 out of the 8 differentially expressed proteins were upregulated **(Figure 8B)**. 22 and 21 differentially expressed cytosolic proteins were downregulated and upregulated, respectively **(Figure 8C)**. GO domain pathways enrichment analysis indicates enrichment of protein binding, cytoplasmic translation, and actin filament organization (with 75, 43, 8, and 8 differentially expressed proteins, respectively). This is consistent with our earlier GO annotation results **(Figure 8D)**.

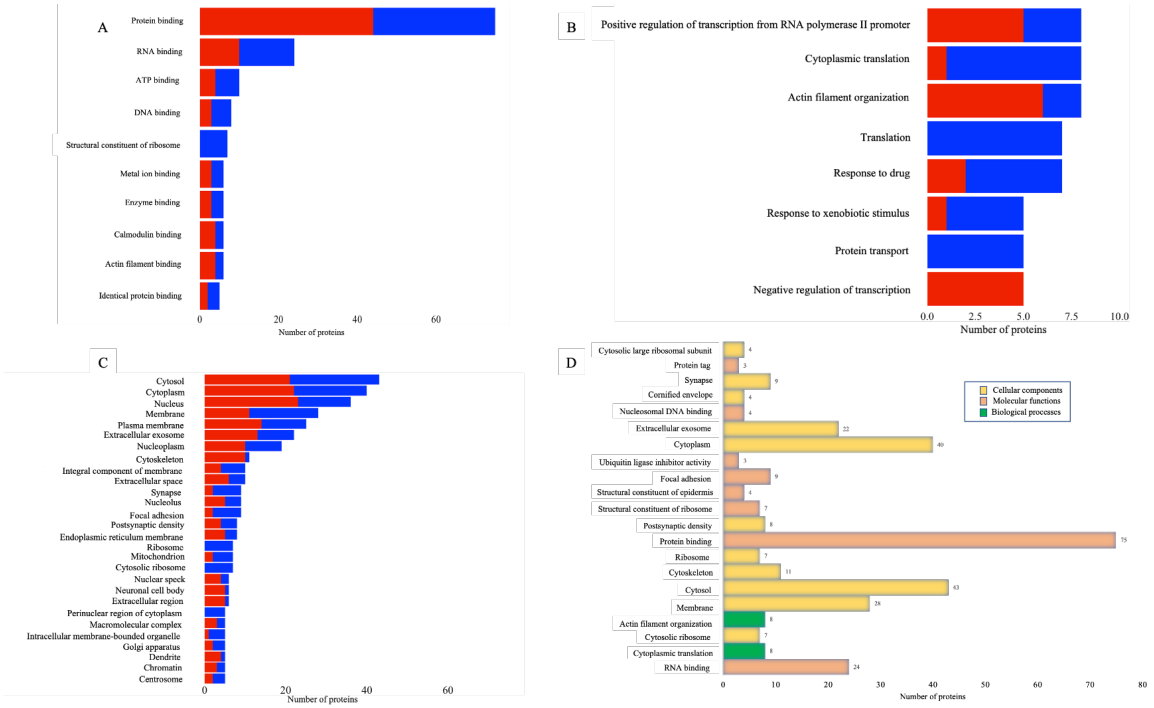

Figure 8: GO domains affected by IMI-olefin treatment of LUHMES cells. Total number of differentially expressed proteins categorized by (A) molecular functions (B) biological processes and (C) cellular components. (D) Enrichment analysis of GO domains affected by the differentially expressed proteins within IMI-olefin treated cells.

3.8. Pathway enrichment analysis of IMI-Olefin treated LUHMES cells

Enrichment analysis using the database of pathways from Reactome shows downregulation of proteins represented in **Table 1**: RPS15, RPS7, RPLP1, RPL36, RPSA, RPL38, and RPL37 in pathways not associated with the "RHO GTPase cycle" **(Figure 9A)**. All of the differentially expressed proteins were downregulated for the "translation" pathway except for EIF4B protein, which was upregulated **(Figure 9A).** KEGG pathways enrichment analysis revealed that all differentially expressed proteins

associated with “ribosomes” are also downregulated, while downregulated PRKCG proteins appear implicated in viral disease as “Coronavirus disease- COVID-19” pathways **(Figure 9B)**. “Cytoplasmic ribosomal proteins” pathways in WikiPathways appear enriched in the dataset and shown as downregulated proteins listed in **Table 1** and **Figure 9C.**

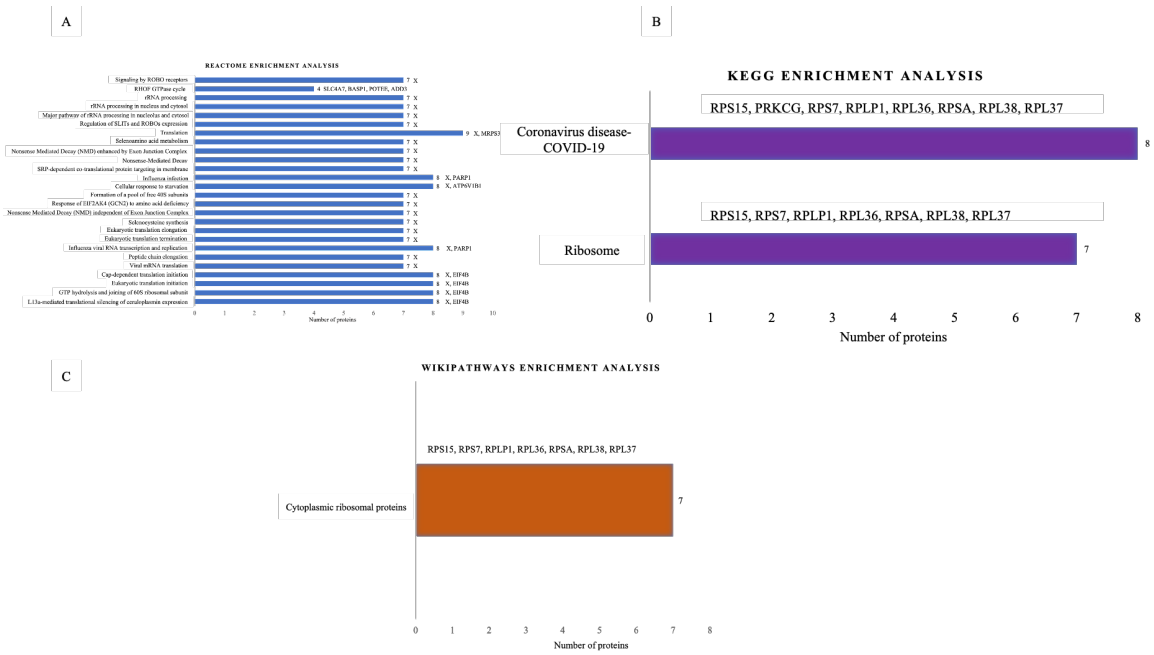

Figure 9: Pathway enrichment analysis of IMI-olefin treated LUHMES cells. (A) Reactome pathways analysis shows proteins in Table 1 marked as "X". (B) KEGG pathways analysis and (C) WikiPathways pathway analysis. The numbers to the left of the bars in each chart represent the number of proteins associated with each Reactome, KEGG, or WikiPathways pathway The proteins associated with each Reactome or WikiPathways pathway were indicated above each bar for B & C and to the right of each bar for A.

Table 1: Ribosomal proteins associated with IMI-Olefin treatment responses.

Table 1	RPS15, RPS7, RPLP1, RPL36, RPSA, RPL38, RPL37

3.9. Convergence of IMI and IMI-olefin proteomic processes on actin regulation

Overlapping proteins are shown using a Venn diagram and indicate differentially expressed proteins upregulated by IMI and IMI-olefin treatment conditions in the LUHMES cell. The 27 proteins that overlap between the two treatment groups are shown in **Figure 10A**. Using DAVID GO enrichment we further examined these 27 overlapping proteins, and this analysis indicates specific enrichment of the proteins in "actin filament organization", "sequestering of actin monomers", and "actin monomer binding" **(Figure 10B)**. Differentially expressed proteins among DN-IMI and IMI-treated cells as well as DN-IMI and IMI-olefin-treated cells show little to no overlap **(Figure 11A-E)**. Notably, 8 overlapping proteins were found to be downregulated by the IMI and IMI-olefin treatment conditions **(Figure 11C)**.

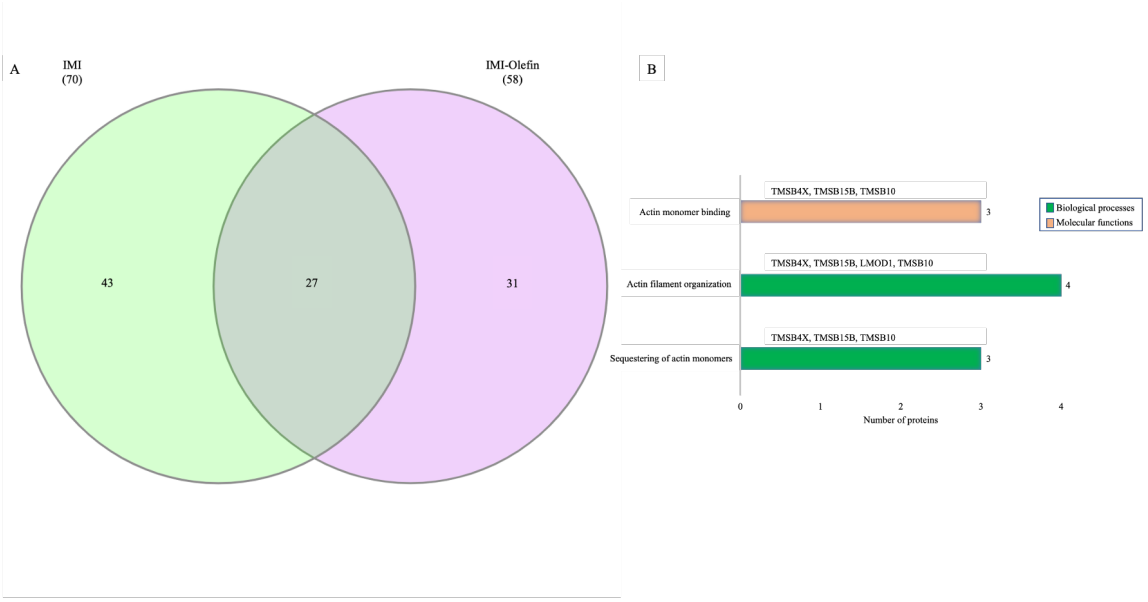

Figure 10: Overlapping proteins found in the IMI and IMI-olefin treatment groups. Venn diagram showing significantly upregulated proteins in IMI and IMI-olefin treated cells. (B) Enrichment analysis of GO domains associated with the overlapping proteins within the IMI and IMI-olefin treatment groups. Venn diagrams were created using the Interactivenn tool **[12]**.

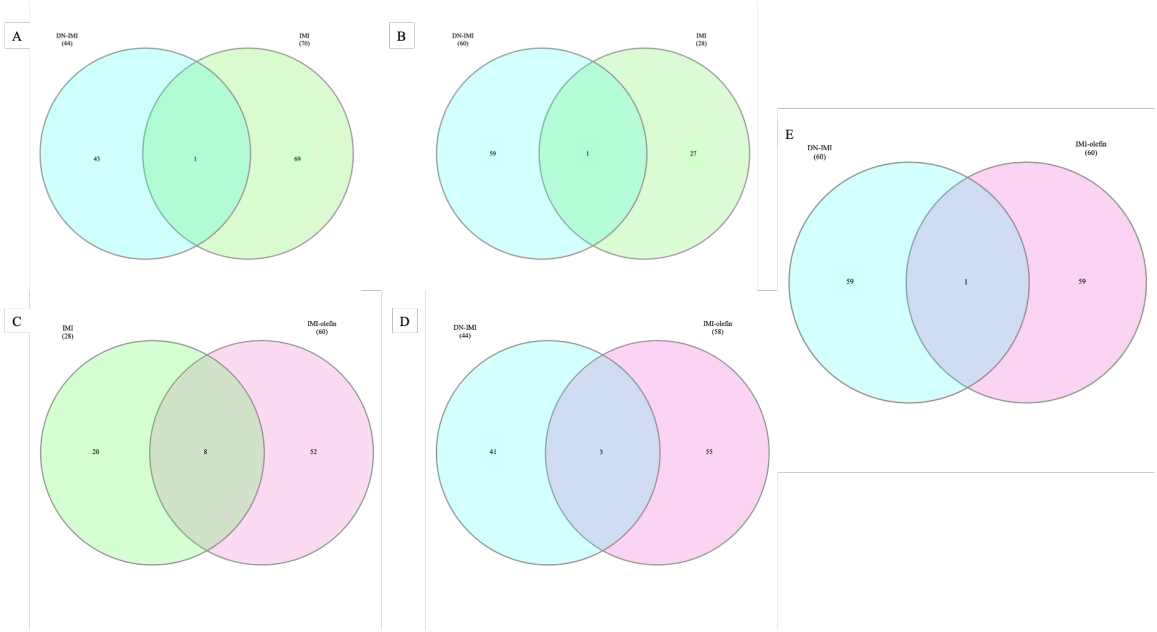

Figure 11: Overlapping proteins in IMI, DN-IMI, and IMI-olefin treatment conditions. (A) Upregulated proteins in DN-IMI and IMI-treated cells (B) Downregulated proteins in DN-IMI and IMI-treated cells (C) Downregulated proteins in IMI and IMI-olefin treated cells (D) Upregulated proteins in DN-IMI and IMI-olefin treated cells (E) Downregulated proteins in DN-IMI and IMI-olefin treated cells.

3.10. DN-IMI and IMI-treated LUHMES cells show higher survival rates

Neonics are known to cause toxicity in various cells and organisms. We wanted to confirm the effects of our non-saturating concentrations on overall cell survival and determine that our proteomic response is not due to cell toxicity/death. To do this we utilized a thresholding and watershed filter tool application within ImageJ that enables semi-automated cell signal analysis within captured images. We used this to determine the number of live *vs*. dead across the IMI and DN-IMI conditions relative to the

controls. At 48 hours of drug treatment, the same time point used for proteomic analysis, we examined calcein-AM and propidium iodide (PI) labeling in LUHMES cells in order to quantify live and dead cells, respectively **(Figure 12A-B)**. As shown in **Figure 12D,** a fluorescent measure across treatment conditions shows that IMI and DN-IMI have no significant effect on total living cell number. However, IMI and DN-IMI treatment was associated with a statistically significant decrease in dead cell (PI) labeling **(Figure 12C)**. These findings suggest that IMI and DN-IMI treatment can impact the mechanism of cell death.

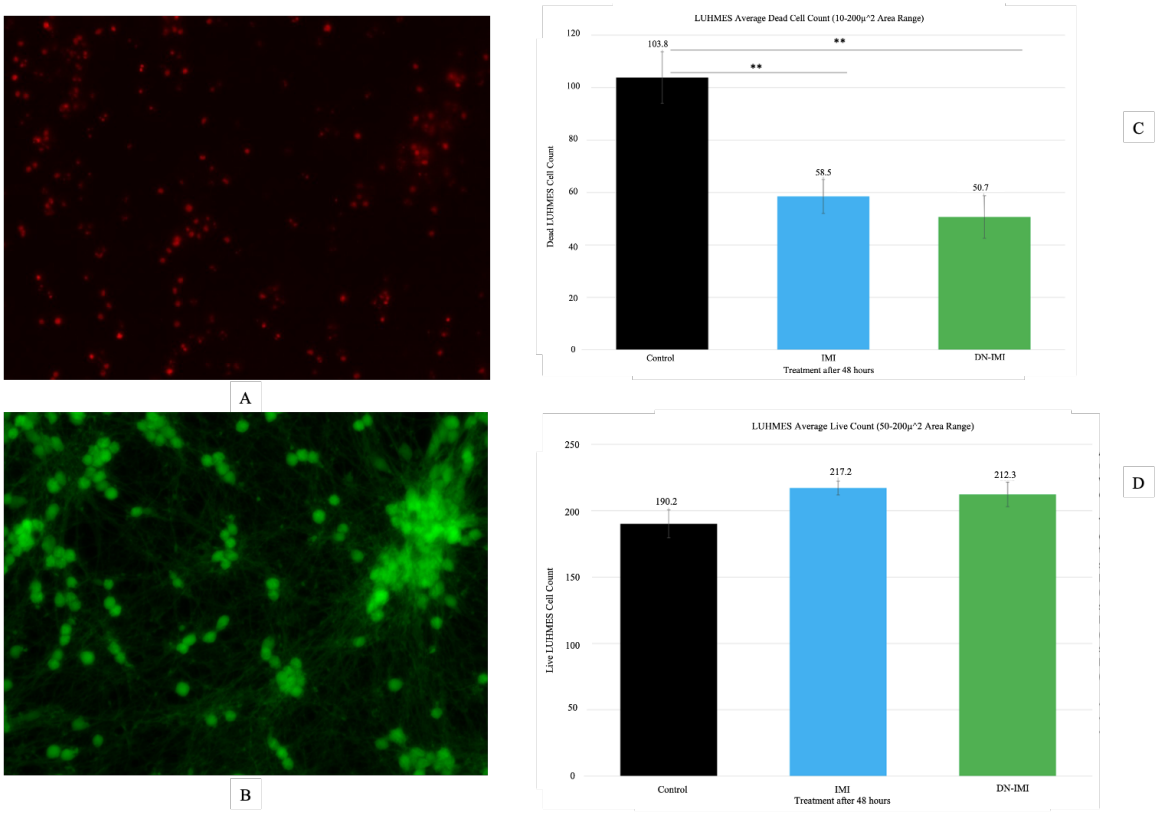

Figure 12: The impact of neonics on cell survival and death. (A) Microscopic image of the propidium iodide (PI) stained LUHMES cells. PI binds to the DNA of dead cells. (B) Microscopic image of the calcein AM stained LUHMES cells. Non-fluorescent calcein AM gets converted to a fluorescent green compound in live cells. (C) Plot of dead cell count in control, DN-IMI, IMI, and IMI-olefin treated LUHMES cells. (D) Plot of live cell count in control, DN-IMI, IMI, and IMI-olefin treated LUHMES cells. The count of the cells was performed using the thresholding and watershed functions of ImageJ. ANOVA one-way analysis using R and assuming equal assumptions was performed. The difference in count between the DN-IMI, IMI, and control was considered statistically significant using alpha as < 0.05. The '**' represents the threshold of statistical significance at p-value less than 0.01.

CHAPTER 4-DISCUSSION

Imidacloprid (IMI) is one of the most widely used neonic class of insecticides in the world and growing evidence points to toxicity against its target (insects) and to varying degrees, off-target organisms including birds and mammals **[4,15,23]**. This effect of IMI is driven by its ability to bind to a highly conserved class of channel nAChR that are abundant across vertebrate and invertebrate species [**15,16,23,27,41]**. IMI is also readily metabolized by enzymes, such as cytochrome P450, and aldehyde oxidase, to produce bioactive products such as IMI-olefin and DN-IMI **[7,8,10,24,32,33,35,38,39,43]**. Studies have shown that IMI and its metabolites DN-IMI and IMI-olefin can bind mammalian nAChRs including α7, α3β4, and α4β2, within the human dopaminergic LUHMES cell line **[24,25]**. Despite evidence for potency against mammalian nAChR, the toxicity mechanisms at cellular and molecular levels underlying DN-IMI and IMI-olefin have not been studied and especially at lower doses that may reflect physiological conditions.

To address this, we used whole-cell proteomics to examine how 2-day (48-hour treatment) of LUHMES cells with 50μM IMI, DN-IMI, and IMI-olefin impact overall protein levels and changes. This concentration is consistent with the ability of these compounds to activate nAChRs in LUHMES cells but does not fully saturate the receptor

site **[24,25]**. Our results show that the total number of differentially expressed proteins in IMI-treated cells compared to controls has increased since we found that more proteins were upregulated than downregulated by IMI treatment. We then analyzed the components of the significantly altered proteins using bioinformatic GO annotation and enrichment analysis. The bioinformatic analysis reveals an effect of IMI on specific processes such as protein binding, a key mechanism for cell signaling, and protein transport within the cytosol. In the context of IMI-mediated protein upregulation, it can be suggested that nAChR activation through IMI increases the synthesis and transport of specific proteins within the cell. Alterations in protein transport have been implicated in various neurodegenerative diseases, and evidence indicates that disruption in protein transport is driven by altered α-synuclein and leucine-rich repeat kinase-2 (LRRK2) functions within mammalian cells during Parkinson's Disease (PD) **[47]**. Cell count analysis using ImageJ indicated a significant reduction in cell death with DN-IMI and IMI-treated LUHMES cells and may suggest that protein upregulation in LUHMES cells may drive important changes in the mechanisms of cell survival.

Whole-cell proteome analysis of DN-IMI treated LUHMES cells illustrated a propensity for drug-related downregulation of protein expression within treated cells as compared to controls. GO annotation and enrichment analysis of significantly altered proteins within the DN-IMI treatment group shows that processes for transcription, apoptosis, and cell proliferation are significantly impacted. This is supported by GO analysis that reveals that altered proteins during DN-IMI are abundant within the nucleus.

Interestingly, apoptotic dysregulation has been suggested to be a driver of neurodegenerative diseases such as PD, Alzheimer's Disease (AD), Huntington's Disease (HD), and Amyotrophic Lateral Sclerosis (ALS) **[9]**. Reactome pathway enrichment analysis of DN-IMI treated cells illustrated the enrichment of differentially expressed proteins in several important cell survival and growth pathways including Wnt, nuclear receptor, ESR-mediated, G protein beta-gamma, and Ras signaling. Pathways such as Wnt and nuclear receptor signaling are specifically dysregulated in neurological disorders **[14,17,26,37]**. Our findings suggest a potential for DN-IMI in Wnt pathway-associated signaling that may lead to long-term neural cell damage. In one scenario, neonic-associated signaling may contribute to the aggregation of amyloid β (Aβ) protein as well as the hyperphosphorylation of tau, as predisposing factors for AD. Studies show that Wnt-associated GSK-3β signaling involving downstream β-catenin activity can directly regulate tau hyperphosphorylation and apoptotic responses leading to synaptotoxicity **[14]**.

Our current findings suggest that the neonics IMI, DN-IMI, and IMI-olefin may impact mechanisms of cell death in LUHMES cells based on proteomics and cell count of PI labeling. However, these findings are still preliminary, and future studies will be needed to confirm the possible role of neonic-mediated Wnt pathway regulation on neuronal cell survival and death. Analysis of the whole-cell proteome in IMI-olefin treated cells suggests that this IMI metabolite significantly impacts both actin-associated processes as well as protein translation through ribosomal regulation. GO enrichment analysis of

overlapping sets of upregulated proteins in IMI and IMI-olefin-treated LUHMES cells, shows a convergence of the two chemical pathways on actin-related cellular processes. Pathway enrichment analysis using KEGG, Reactome, and WikiPathways databases revealed that several pathways for protein translation are affected via a cohort of specific ribosomal proteins. Interestingly, studies in honeybees have shown that sublethal doses of IMI can also impact ribosomal translation and actin-related processes **[48]**. Thus, our proteomic findings in human neural cells may reveal a conserved mechanism for neonic actions across species. Within mammals, studies indicate that repression of protein translation may contribute to neurodegenerative disorders such as ALS and Frontotemporal Dementia (FTD) **[2]**. Overall, the proteomic and bioinformatic analysis performed here on LUHMES cells treated with non-saturating levels of IMI and its primary metabolites DN-IMI and IMI-olefin illustrates an impact of these chemical agents on important biological processes in human cells. Specifically, the data supports the hypothesis that IMI and its metabolites can disrupt cellular homeostasis through changes in gene transcription, protein translation, mechanism of proliferation/survival, and apoptosis. Many such pathways appear disrupted in neurodegenerative disease and suggest that neonic toxicity may serve as a contributing factor for neuro disease onset/progression. Based on these findings, as well as existing evidence for the ability of IMI and its metabolites to bind and activate mammalian nAChRs **[24,25]**, it is important to further understand the long-term impact of these chemicals on human health.

REFERENCES

1. Abou-Donia, M. B., Goldstein, L. B., Bullman, S., Tu, T., Khan, W. A., Dechkovskaia, A. M., & Abdel-Rahman, A. A. (2008). Imidacloprid Induces Neurobehavioral Deficits and Increases Expression of Glial Fibrillary Acidic Protein in the Motor Cortex and Hippocampus in Offspring Rats Following in Utero Exposure. *Journal of Toxicology and Environmental Health, Part A*, *71*(2), 119–130. https://doi.org/10.1080/15287390701613140
2. Bosco D. A. (2018). Translation dysregulation in neurodegenerative disorders. *Proceedings of the National Academy of Sciences of the United States of America*, *115*(51), 12842–12844. https://doi.org/10.1073/pnas.1818493115
3. Calderón-Segura, M. E., Gómez-Arroyo, S., Villalobos-Pietrini, R., Martínez-Valenzuela, C., Carbajal-López, Y., Calderón-Ezquerro, M. del C., Cortés-Eslava, J., García-Martínez, R., Flores-Ramírez, D., Rodríguez-Romero, M. I., Méndez-Pérez, P., & Bañuelos-Ruíz, E. (2012). Evaluation of Genotoxic and Cytotoxic Effects in Human Peripheral Blood Lymphocytes Exposed In Vitro to Neonicotinoid Insecticides News. *Journal of Toxicology*, *2012*, e612647. https://doi.org/10.1155/2012/612647
4. Chen, M., Tao, L., McLean, J., & Lu, C. (2014). Quantitative Analysis of Neonicotinoid Insecticide Residues in Foods: Implication for Dietary Exposures.

Journal of Agricultural and Food Chemistry, *62*(26), 6082–6090. https://doi.org/10.1021/jf501397m

5. Cimino, A. M., Boyles, A. L., Thayer, K. A., & Perry, M. J. (2017). Effects of Neonicotinoid Pesticide Exposure on Human Health: A Systematic Review. *Environmental Health Perspectives*, *125*(2), 155–162. https://doi.org/10.1289/EHP515
6. Codling, G., Al Naggar, Y., Giesy, J. P., & Robertson, A. J. (2016). Concentrations of neonicotinoid insecticides in honey, pollen and honey bees (Apis mellifera L.) in central Saskatchewan, Canada.Chemosphere, *144*, 2321–2328. https://doi.org/10.1016/j.chemosphere.2015.10.135
7. Dick, R. A., Kanne, D. B., & Casida, J. E. (2005). Identification of aldehyde oxidase as the neonicotinoid nitroreductase. *Chemical research in toxicology*, *18*(2), 317–323. https://doi.org/10.1021/tx049737i
8. Ford, K. A., & Casida, J. E. (2006). Chloropyridinyl Neonicotinoid Insecticides: Diverse Molecular Substituents Contribute to Facile Metabolism in Mice. *Chemical Research in Toxicology*, *19*(7), 944–951. https://doi.org/10.1021/tx0600696
9. Ghavami, S., Shojaei, S., Yeganeh, B., Ande, S. R., Jangamreddy, J. R., Mehrpour, M., Christoffersson, J., Chaabane, W., Moghadam, A. R., Kashani, H. H., Hashemi, M., Owji, A. A., & Łos, M. J. (2014). Autophagy and apoptosis dysfunction in neurodegenerative disorders. *Progress in neurobiology*, *112*, 24–49. https://doi.org/10.1016/j.pneurobio.2013.10.004

10. Goulson, D. (2013). REVIEW: An overview of the environmental risks posed by neonicotinoid insecticides. *Journal of Applied Ecology*, *50*(4), 977–987. https://doi.org/10.1111/1365-2664.12111

11. Gu, Y., Li, Y., Huang, X., Zheng, J., Yang, J., Diao, H., Yuan, Y., Xu, Y., Liu, M., Shi, H., & Xu, W. (2013). Reproductive Effects of Two Neonicotinoid Insecticides on Mouse Sperm Function and Early Embryonic Development In Vitro. *PLOS ONE*, *8*(7), e70112. https://doi.org/10.1371/journal.pone.0070112

12. Heberle, H., Meirelles, G. V., da Silva, F. R., Telles, G. P., & Minghim, R. (2015). InteractiVenn: a web-based tool for the analysis of sets through Venn diagrams. *BMC bioinformatics*, *16*(1), 169. https://doi.org/10.1186/s12859-015-0611-3

13. Hirano, T., Minagawa, S., Furusawa, Y., Yunoki, T., Ikenaka, Y., Yokoyama, T., Hoshi, N., & Tabuchi, Y. (2019). Growth and neurite stimulating effects of the neonicotinoid pesticide clothianidin on human neuroblastoma SH-SY5Y cells. *Toxicology and Applied Pharmacology*, *383*, 114777. https://doi.org/10.1016/j.taap.2019.114777

14. Inestrosa, N. C., & Toledo, E. M. (2008). The role of Wnt signaling in neuronal dysfunction in Alzheimer's Disease. *Molecular neurodegeneration*, *3*, 9. https://doi.org/10.1186/1750-1326-3-9

15. Jeschke, P., Nauen, R., Schindler, M., & Elbert, A. (2011). Overview of the status and global strategy for neonicotinoids. *Journal of agricultural and food chemistry*, *59*(7), 2897–2908. https://doi.org/10.1021/jf101303g

16. Kimura-Kuroda, J., Komuta, Y., Kuroda, Y., Hayashi, M., & Kawano, H. (2012). Nicotine-Like Effects of the Neonicotinoid Insecticides Acetamiprid and Imidacloprid on Cerebellar Neurons from Neonatal Rats. *PLOS ONE*, *7*(2), e32432. https://doi.org/10.1371/journal.pone.0032432
17. Kirouac, L., Rajic, A. J., Cribbs, D. H., & Padmanabhan, J. (2017). Activation of Ras-ERK Signaling and GSK-3 by Amyloid Precursor Protein and Amyloid Beta Facilitates Neurodegeneration in Alzheimer's Disease. *eNeuro*, *4*(2), ENEURO.0149-16.2017. https://doi.org/10.1523/ENEURO.0149-16.2017
18. Klarich, K. L., Pflug, N. C., DeWald, E. M., Hladik, M. L., Kolpin, D. W., Cwiertny, D. M., & LeFevre, G. H. (2017). Occurrence of Neonicotinoid Insecticides in Finished Drinking Water and Fate during Drinking Water Treatment. *Environmental Science & Technology Letters*, *4*(5), 168–173. https://doi.org/10.1021/acs.estlett.7b00081
19. Klarich Wong, K. L., Webb, D. T., Nagorzanski, M. R., Kolpin, D. W., Hladik, M. L., Cwiertny, D. M., & LeFevre, G. H. (2019). Chlorinated Byproducts of Neonicotinoids and Their Metabolites: An Unrecognized Human Exposure Potential? *Environmental Science & Technology Letters*, *6*(2), 98–105. https://doi.org/10.1021/acs.estlett.8b00706
20. Kollmeyer, W. D., Flattum, R. F., Foster, J. P., Powell, J. E., Schroeder, M. E., & Soloway, S. B. (1999). Discovery of the Nitromethylene Heterocycle Insecticides. In I. Yamamoto & J. E. Casida (Eds.), *Nicotinoid Insecticides and the Nicotinic*

Acetylcholine Receptor (pp. 71–89). Springer Japan. https://doi.org/10.1007/978-4-431-67933-2_3

21. Krug, A. K., Balmer, N. V., Matt, F., Schönenberger, F., Merhof, D., & Leist, M. (2013). Evaluation of a human neurite growth assay as specific screen for developmental neurotoxicants. *Archives of Toxicology*, *87*(12), 2215–2231. https://doi.org/10.1007/s00204-013-1072-y
22. Laubscher, B., Diezi, M., Renella, R., Mitchell, E. A. D., Aebi, A., Mulot, M., & Glauser, G. (2022). Multiple neonicotinoids in children's cerebro-spinal fluid, plasma, and urine. *Environmental Health*, *21*(1), 10. https://doi.org/10.1186/s12940-021-00821-z
23. Lin, P.-C., Lin, H.-J., Liao, Y.-Y., Guo, H.-R., & Chen, K.-T. (2013). Acute Poisoning with Neonicotinoid Insecticides: A Case Report and Literature Review. *Basic & Clinical Pharmacology & Toxicology*, *112*(4), 282–286. https://doi.org/10.1111/bcpt.12027
24. Loser, D., Grillberger, K., Hinojosa, M. G., Blum, J., Haufe, Y., Danker, T., Johansson, Y., Möller, C., Nicke, A., Bennekou, S. H., Gardner, I., Bauch, C., Walker, P., Forsby, A., Ecker, G. F., Kraushaar, U., & Leist, M. (2021). Acute effects of the imidacloprid metabolite desnitro-imidacloprid on human nACh receptors relevant for neuronal signaling. *Archives of Toxicology*, *95*(12), 3695–3716. https://doi.org/10.1007/s00204-021-03168-z
25. Loser, D., Hinojosa, M. G., Blum, J., Schaefer, J., Brüll, M., Johansson, Y., Suciu, I., Grillberger, K., Danker, T., Möller, C., Gardner, I., Ecker, G. F.,

Bennekou, S. H., Forsby, A., Kraushaar, U., & Leist, M. (2021). Functional alterations by a subgroup of neonicotinoid pesticides in human dopaminergic neurons. *Archives of Toxicology*, *95*(6), 2081–2107. https://doi.org/10.1007/s00204-021-03031-1

26. Marchetti B. (2018). Wnt/β-Catenin Signaling Pathway Governs a Full Program for Dopaminergic Neuron Survival, Neurorescue and Regeneration in the MPTP Mouse Model of Parkinson's Disease. *International journal of molecular sciences*, *19*(12), 3743. https://doi.org/10.3390/ijms19123743
27. Martelli, F., Zhongyuan, Z., Wang, J., Wong, C. O., Karagas, N. E., Roessner, U., Rupasinghe, T., Venkatachalam, K., Perry, T., Bellen, H. J., & Batterham, P. (2020). Low doses of the neonicotinoid insecticide imidacloprid induce ROS triggering neurological and metabolic impairments in *Drosophila*. *Proceedings of the National Academy of Sciences of the United States of America*, *117*(41), 25840–25850. https://doi.org/10.1073/pnas.2011828117
28. Nadine Kabbani. (2022, May 4). *Cell Count Using ImageJ*. https://www.youtube.com/watch?v=De2wmWKPmCA
29. Nauen, R., Reckmann, U., Armborst, S., Stupp, H.-P., & Elbert, A. (1999). Whitefly-active metabolites of imidacloprid: Biological efficacy and translocation in cotton plants. *Pesticide Science*, *55*(3), 265–271. https://doi.org/10.1002/(SICI)1096-9063(199903)55:3<265::AID-PS891>3.0.CO;2-C

30. Schildknecht, S., Karreman, C., Pöltl, D., Efrémova, L., Kullmann, C., Gutbier, S., Krug, A., Scholz, D., Gerding, H. R., & Leist, M. (2013). Generation of genetically-modified human differentiated cells for toxicological tests and the study of neurodegenerative diseases. *ALTEX - Alternatives to Animal Experimentation*, *30*(4), 427–444. https://doi.org/10.14573/altex.2013.4.427
31. Scholz, D., Pöltl, D., Genewsky, A., Weng, M., Waldmann, T., Schildknecht, S., & Leist, M. (2011). Rapid, complete and large-scale generation of post-mitotic neurons from the human LUHMES cell line. *Journal of Neurochemistry*, *119*(5), 957–971. https://doi.org/10.1111/j.1471-4159.2011.07255.x
32. Schulz-Jander, D. A., & Casida, J. E. (2002). Imidacloprid insecticide metabolism: human cytochrome P450 isozymes differ in selectivity for imidazolidine oxidation versus nitroimine reduction. *Toxicology letters*, *132*(1), 65–70. https://doi.org/10.1016/s0378-4274(02)00068-1
33. Schulz-Jander, D. A., Leimkuehler, W. M., & Casida, J. E. (2002). Neonicotinoid insecticides: reduction and cleavage of imidacloprid nitroimine substituent by liver microsomal and cytosolic enzymes. *Chemical research in toxicology*, *15*(9), 1158–1165. https://doi.org/10.1021/tx0200360
34. Shadnia, S., & Moghaddam, H. H. (2008). Fatal intoxication with imidacloprid insecticide. *The American Journal of Emergency Medicine*, *26*(5), 634.e1-634.e4. https://doi.org/10.1016/j.ajem.2007.09.024
35. Simon-Delso, N., Amaral-Rogers, V., Belzunces, L. P., Bonmatin, J. M., Chagnon, M., Downs, C., Furlan, L., Gibbons, D. W., Giorio, C., Girolami, V.,

Goulson, D., Kreutzweiser, D. P., Krupke, C. H., Liess, M., Long, E., McField, M., Mineau, P., Mitchell, E. A., Morrissey, C. A., Noome, D. A., … Wiemers, M. (2015). Systemic insecticides (neonicotinoids and fipronil): trends, uses, mode of action and metabolites. *Environmental science and pollution research international*, *22*(1), 5–34. https://doi.org/10.1007/s11356-014-3470-y

36. Sinclair, P., Baranova, A., & Kabbani, N. (2021). Mitochondrial Disruption by Amyloid Beta 42 Identified by Proteomics and Pathway Mapping. *Cells*, *10*(9), 2380. https://doi.org/10.3390/cells10092380
37. Skerrett, R., Malm, T., & Landreth, G. (2014). Nuclear receptors in neurodegenerative diseases. *Neurobiology of disease*, *72 Pt A*, 104–116. https://doi.org/10.1016/j.nbd.2014.05.019
38. Swenson, T. L., & Casida, J. E. (2013). Aldehyde Oxidase Importance In Vivo in Xenobiotic Metabolism: Imidacloprid Nitroreduction in Mice. *Toxicological Sciences*, *133*(1), 22–28. https://doi.org/10.1093/toxsci/kft066
39. Thompson, D. A., Lehmler, H.-J., Kolpin, D. W., Hladik, M. L., Vargo, J. D., Schilling, K. E., LeFevre, G. H., Peeples, T. L., Poch, M. C., LaDuca, L. E., Cwiertny, D. M., & Field, R. W. (2020). A critical review on the potential impacts of neonicotinoid insecticide use: Current knowledge of environmental fate, toxicity, and implications for human health. *Environmental Science: Processes & Impacts*, *22*(6), 1315–1346. https://doi.org/10.1039/C9EM00586B
40. Tomizawa, M., & Casida, J. E. (2000). Imidacloprid, Thiacloprid, and Their Imine Derivatives Up-Regulate the α4β2 Nicotinic Acetylcholine Receptor in

M10 Cells. *Toxicology and Applied Pharmacology*, *169*(1), 114–120. https://doi.org/10.1006/taap.2000.9057

41. Tomizawa, M., & Casida, J. E. (2005). NEONICOTINOID INSECTICIDE TOXICOLOGY: Mechanisms of Selective Action. *Annual Review of Pharmacology and Toxicology*, *45*(1), 247–268. https://doi.org/10.1146/annurev.pharmtox.45.120403.095930
42. *USGS NAWQA: The Pesticide National Synthesis Project*. (n.d.). Retrieved June 2, 2022, from https://water.usgs.gov/nawqa/pnsp/usage/maps/show_map.php?year=2014&map=IMIDACLOPRID&hilo=L
43. Vardavas, A. I., Ozcagli, E., Fragkiadaki, P., Stivaktakis, P. D., Tzatzarakis, M. N., Alegakis, A. K., Vasilaki, F., Kaloudis, K., Tsiaoussis, J., Kouretas, D., Tsitsimpikou, C., Carvalho, F., & Tsatsakis, A. M. (2018). The metabolism of imidacloprid by aldehyde oxidase contributes to its clastogenic effect in New Zealand rabbits. *Mutation research. Genetic toxicology and environmental mutagenesis*, *829-830*, 26–32. https://doi.org/10.1016/j.mrgentox.2018.03.002
44. Vinod, K. V., Srikant, S., Thiruvikramaprakash, G., & Dutta, T. K. (2015). A fatal case of thiacloprid poisoning. *The American Journal of Emergency Medicine*, *33*(2), 310.e5-310.e6. https://doi.org/10.1016/j.ajem.2014.08.013
45. Wan, Y., Han, Q., Wang, Y., & He, Z. (2020). Five degradates of imidacloprid in source water, treated water, and tap water in Wuhan, central China. *Science of*

The Total Environment, *741*, 140227. https://doi.org/10.1016/j.scitotenv.2020.140227

46. Wang, A., Mahai, G., Wan, Y., Yang, Z., He, Z., Xu, S., & Xia, W. (2020). Assessment of imidacloprid related exposure using imidacloprid-olefin and desnitro-imidacloprid: Neonicotinoid insecticides in human urine in Wuhan, China. *Environment International*, *141*, 105785. https://doi.org/10.1016/j.envint.2020.105785
47. Wang, X., Huang, T., Bu, G., & Xu, H. (2014). Dysregulation of protein trafficking in neurodegeneration. *Molecular neurodegeneration*, *9*, 31. https://doi.org/10.1186/1750-1326-9-31
48. Wu, Y. Y., Luo, Q. H., Hou, C. S., Wang, Q., Dai, P. L., Gao, J., Liu, Y. J., & Diao, Q. Y. (2017). Sublethal effects of imidacloprid on targeting muscle and ribosomal protein related genes in the honey bee Apis mellifera L. *Scientific reports*, *7*(1), 15943. https://doi.org/10.1038/s41598-017-16245-0
49. Zhang, X., Yin, M., & Zhang, M. (2014). Cell-based assays for Parkinson's disease using differentiated human LUHMES cells. *Acta Pharmacologica Sinica*, *35*(7), 945–956. https://doi.org/10.1038/aps.2014.36

BIOGRAPHY

Sreehari Girish Kumar graduated from George C. Marshall High School, Falls Church, Virginia, in 2016. He received his Bachelor of Science in Neuroscience from George Mason University in 2020. He will be graduating with a Master of Science in Biology from George Mason University in Summer 2022. He will be attending University of Alabama in Birmingham for his Ph.D. in Cellular and Molecular biology in Fall 2022.